Inorganic Chemistry

Article

Cite This: Inorg. Chem. 2019, 58, 8151−8161

pubs.acs.org/IC

Group 9 and 10 Metal Complexes of an Ylide-Substituted Phosphine: Coordination versus Cyclometalation and Oxidative Addition

Thorsten Scherpf, Ilja Rodstein, Maurice Paaßen, and Viktoria H. Gessner*

Chair of Inorganic Chemistry II, Ruhr-Universität Bochum, Universitätsstraße 150, 44801 Bochum, Germany

Supporting Information

ABSTRACT: Ylide-substituted phosphines (YPhos) have been shown to be excellent ligands for several transition metal catalyzed reactions. Investigations of the coordination behavior of the YPhos ligand Y_SPPh_2 (**1**) [with Y_S = $(Ph_3P)(SO_2Tol)C$] toward group 9 and 10 metals revealed a surprisingly diverse coordination chemistry of the ligand. With $Ni(CO)_4$, the formation of a di- as well as tricarbonyl complex is observed depending on the reaction conditions. In $[(\kappa P,\eta^2\text{-benzene-}\mathbf{1})Ni(CO)_2]$ the phosphine ligand also coordinates via a phosphonium bound phenyl group to the metal leading to a unique nickel η^2-arene interaction, which can be viewed as an intermediate state toward P−C bond activation. Full cleavage of the P−C bond takes place with $[Rh(COD)Cl]_2$ leading to a complex salt with $[(\kappa P,\kappa O\text{-}\mathbf{1})Rh(COD)]^+$ as cation and a dirhodium trichloride complex anion. Here, Y_SPPh_2 underwent P−C bond cleavage to thus act as an anionic diphosphine ligand. In contrast, in $[(\kappa P,\kappa O\text{-}\mathbf{1})Rh(COD)]^+$ as well as $[(\kappa P,\kappa O\text{-}\mathbf{1})Rh(CO)Cl]$, formed from the reaction of **1** with $[Rh(CO)_2Cl]_2$, the YPhos ligand acts as bidentate ligand complexing the metal via the phosphine and sulfonyl moiety with an intact PPh_3 unit. A further type of coordination is observed with $[Ir(COD)Cl]_2$. Here, phosphine coordination is accompanied by C−H activation at one of the phosphonium bound phenyl groups leading to a cyclometalated complex.

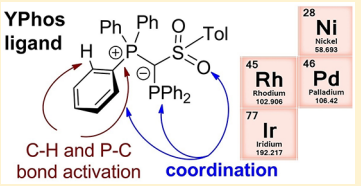

INTRODUCTION

Phosphines are ubiquitous in coordination chemistry and homogeneous catalysis. For many decades, their further development by changing the electronic and steric properties has been part of vivid research activities.[1] While monophosphines are typically considered as simple L donor ligands, their coordination chemistry can be quite versatile. Depending on the ligand architecture, the phosphine coordination can be accompanied by further ligand metal interactions. In the simplest case, this might be the coordination of further donor sites in the ligand system. However, also cyclometalation processes—typically via C−H activation of an adjacent phenyl group—have often been observed for aryl phosphines[2] and are frequently used for the synthesis of pincer complexes.[3,4] Furthermore, P−C bond splitting reactions have been reported particularly at electron-deficient metal species[5] and also catalytically been applied in coupling reactions.[6] Here, usually the formation of an intermediate phosphonium species is involved.

Recently, we reported on ylide-substituted phosphines (YPhos), formed by incorporation of an ylide group directly at the phosphorus center.[7] Due to the strong electron donation from the ylide these phosphines become more electron-rich than classical phosphines with donor strengths comparable to those of *N*-heterocyclic carbenes.[8] The YPhos ligands turned out to be ideal supporting ligands for transition metal catalysts and showed excellent performance in gold catalyzed hydroamination reactions as well as Buchwald Hartwig aminations under mild reaction conditions.[9] Besides their remarkable donor strength, the unique architecture of the phosphines was found to be decisive for their activity. In case of palladium catalysis, an agostic interaction between the metal and a cyclohexyl group of a PCy_3 phosphonium moiety was observed in the catalytically active species, resulting in a further stabilization of the complex. In gold catalysis with the triphenylphosphonium substituted ligands, however, we suggested the presence of a stabilizing Au-arene interaction similar to the Buchwald-type biarylphophine ligands.[10] These observations suggested a rich coordination chemistry of these PPh_3 substituted YPhos ligands (Figure 1), which we set out to further explore.

RESULTS AND DISCUSSIONS

We started our investigations with the sulfonyl-functionalized YPhos ligand Y_SPPh_2 (**1**), which showed a high activity in gold catalysis. We particularly focused on group 9 and 10 metals due to their importance in homogeneous catalysis. Preliminary attempts to determine the Tolman electronic parameter of **1**

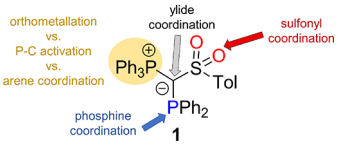

Figure 1. Possible coordination and reactive sites in the ylide-functionalized phosphine **1**.

Received: April 1, 2019
Published: June 5, 2019

DOI: 10.1021/acs.inorgchem.9b00948
Inorg. Chem. 2019, 58, 8151−8161

via synthesis of the corresponding nickel tricarbonyl complex gave no reliable data.[7] Thus, the isolation of the corresponding complex was attempted. Treatment of Y_SPPh_2 with 1 equiv of $[Ni(CO)_4]$ at first resulted in the expected formation of the complex $[(\kappa P\text{-}\mathbf{1})Ni(CO)_3]$ as evidenced by NMR spectroscopy (Scheme 1). As such, two new doublets were observed in

Scheme 1. Preparation of Nickel Carbonyl Complexes of Y_SPPh_2 (1) and Y_SPMe_2 (2)

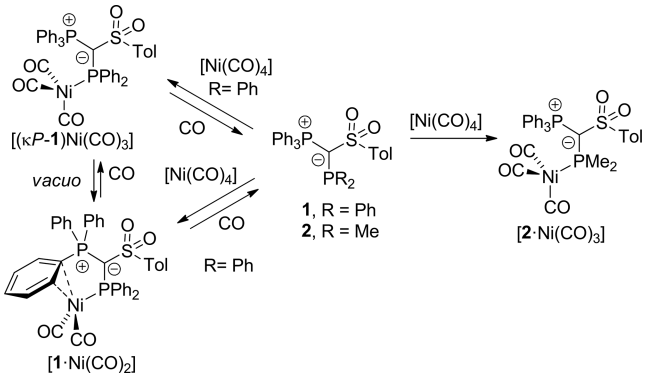

the $^{31}P\{^1H\}$ NMR spectrum at δ_P = 18.6 and 20.7 ppm with a coupling constant of $^2J_{PP}$ = 54.6 Hz. However, removal of the solvent *in vacuo* resulted in the disappearance of these signals and the appearance of a new, somewhat broadened signal at 23.8 ppm, which we assigned to a dicarbonyl complex. Remarkably, this reaction revealed to be reversible. Applying an atmosphere of CO resulted in the reformation of $[(\kappa P\text{-}\mathbf{1})Ni(CO)_3]$ and the appearance of its corresponding two doublets in the $^{31}P\{^1H\}$ NMR spectrum. At higher CO pressures even the cleavage of the phosphine ligand and reformation of $[Ni(CO)_4]$ was observed. Due to the equilibrium and further decomposition of $[\mathbf{1}\cdot Ni(CO)_2]$ no full characterization of the complexes was possible. However, crystallization allowed the isolation of both complexes in the solid state (Figure 2). Diffusion of pentane into a benzene solution gave way to the nickel dicarbonyl complex, while crystallization under a CO atmosphere allowed the isolation of $[(\kappa P\text{-}\mathbf{1})Ni(CO)_3]$. Both molecular structures are depicted in Figure 1 (monoclinic space group $P2_1/c$). While the tricarbonyl complex shows the expected coordination of the YPhos ligand solely via the phosphine unit, the dicarbonyl complex features an additional η^2-coordination of the nickel atom by one of the phenyl groups of the triphenylphosphonium moiety. The structure of $[(\kappa P,\eta^2\text{-benzene-}\mathbf{1})Ni(CO)_2]$ ($[\mathbf{1}\cdot Ni(CO)_2]$) contains two molecules in the asymmetric unit, which both feature the same coordination mode. To the best of our knowledge such a secondary arene interaction with an aryl phosphonium moiety has never been observed for nickel.[11] This interaction in $[\mathbf{1}\cdot Ni(CO)_2]$ becomes evident from short Ni–C interactions to the *ipso* and *ortho* carbon atoms, which range between 2.243(2) and 2.404(2) Å. It is interesting to note that the two molecules in the asymmetric unit show quite different Ni–C distances, which suggests that the interaction is only weak and sensitive to packing effects. Due to the Ni arene interaction the involved C–C bond is slightly elongated (1.415(2) and 1.403(2) Å) in comparison to the other C–C bonds in the phenyl groups (approximately 1.39 Å). The arene Ni interaction also results in a distinct bending of the phenyl ring which becomes evident from the C–C–C-P dihedral angle of 167.4(2)° and 159.9(2)°, which clearly differs from the ideal 180°. The P2–Ni distances of 2.233(1) and 2.215(1) Å are comparable to those for reported nickel(0) phosphine complexes.[12]

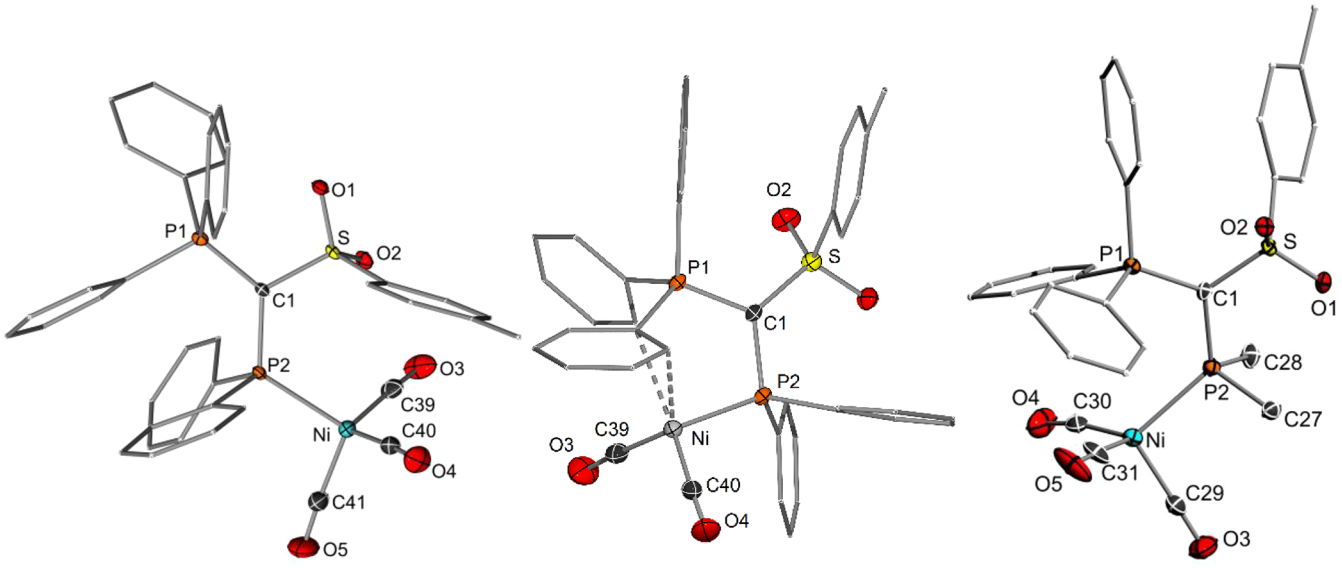

Figure 2. Molecular structures of the nickel carbonyl complexes of Y_SPPh_2 (**1**) and Y_SPMe_2 (**2**). Hydrogen atoms and solvent molecules are omitted for clarity; only one of the two molecules in the asymmetric unit is shown. Displacement parameters at the 50% level. Selected bond lengths [Å] and angles [deg]: $[\mathbf{1}\cdot Ni(CO)_3]$, Ni–C41 1.794(2), Ni–C39 1.806(2), Ni–C40 1.806(2), Ni–P2 2.2588(5), C1–S 1.7131(16), C1–P1 1.7431(17), C1–P2 1.7945(16), S(1)–C(1)–P(1) 112.51(9); $[\mathbf{1}\cdot Ni(CO)_2]$, P(1)–C(1) 1.7342(15), S(1)–C(1) 1.7130(16), C(1)–P(2) 1.7704(16), Ni(1)–P(2) 2.2149(5), Ni(1)–C(9) 2.2426(15), Ni(1)–C(10) 2.2814(15), C(9)–C(10) 1.415(2), S(1)–C(1)–P(2) 118.39(9), P(1)–C(1)–P(2) 116.46(9). **2**·$[Ni(CO)_3]$, P(1)–C(1) 1.729(4), S(1)–C(1) 1.726(4), C(1)–P(2) 1.807(4), Ni(1)–P(2) 2.2737(13), Ni(1)–C(29) 1.795(5), Ni(1)–C(30) 1.806(6), Ni(1)–C(31) 1.783(6), O(3)–C(29) 1.134(6), O(4)–C(30) 1.137(6), O(5)–C(31) 1.144(6), S(1)–C(1)–P(1) 118.4(2), P(1)–C(1)–P(2) 119.1(2).

DOI: 10.1021/acs.inorgchem.9b00948
Inorg. Chem. 2019, 58, 8151–8161

In contrast to Y_SPPh_2, the less bulky methyl-substituted ligand Y_SPMe_2 (**2**) selectively gives way to the tricarbonyl complex $[(\kappa P\text{-}Y_SPMe_2)Ni(CO)_3]$ upon treatment with $Ni(CO)_4$ (Scheme 1). No further loss of CO was observed, even upon drying of the solid in vacuo. $[(\kappa P\text{-}\mathbf{2})Ni(CO)_3]$ could be isolated as yellow solid in 61% yield and fully characterized. The complex exhibits two sharp doublets at −11.8 and +20.3 ppm with a coupling constant of 75.7 Hz in the $^{31}P\{^1H\}$ NMR spectrum. The signal of the carbon atom of the carbonyl ligands resonates at 196.2 ppm, in the typical range of known terminal nickel carbonyls.[13] The CO stretching frequency of 2060.2 cm^{-1} determined by IR spectroscopy confirms the strong donor property of the YPhos ligand, as recently reported based on the [LRh(acac)Cl] complex.[7] The stronger donor property of **2** compared to **1** (TEP(**1**) = 2066.5 cm^{-1}) is probably also the reason for the selective formation of the tricarbonyl complex. Due to the resulting higher electron density at nickel the carbonyl ligands should be stronger bound in $[(\kappa P\text{-}\mathbf{2})Ni(CO)_3]$ than in $[(\kappa P\text{-}\mathbf{1})Ni(CO)_3]$ and thus more difficult to be replaced by arene coordination. Single crystals of $[(\kappa P\text{-}\mathbf{2})Ni(CO)_3]$ were obtained by diffusion of hexane into a benzene solution (Figure 2). The complex crystallizes in the monoclinic space group *C*/*c* with two molecules in the asymmetric unit. In the structure of $[(\kappa P\text{-}\mathbf{2})Ni(CO)_3]$, the YPhos ligand adopts a *syn*-arrangement with the $[Ni(CO)_3]$ fragment being oriented on the same side as the bulky PPh_3 moiety (Figure 3). This results in steric congestion, which becomes evident from the structural parameters. As such, the geometry around the nickel atom strongly deviates from an ideal tetrahedron with the angles around nickel ranging from 99.7(2) to 116.5(2)°. The Ni−P distance of 2.2737(13) Å is the longest in the series of compounds despite the smaller size of the ligand itself (% V_{bur}(**1**) = 49.6; % V_{bur}(**2**) = 46.2). In contrast, an antiarrangement is observed in $[(\kappa P\text{-}\mathbf{1})Ni(CO)_3]$ in the solid state.

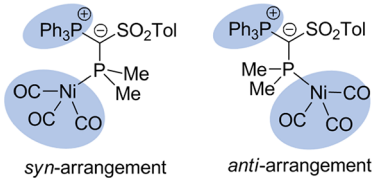

Figure 3. *syn*- and *anti*-conformers for $[(\kappa P\text{-}\mathbf{2})Ni(CO)_3]$.

It is so far unclear why the nickel complex of the Y_sPMe_2 ligand prefers the *syn*-arrangement in the solid state, while its phenyl analogue prefers the *anti*-conformer. It is likely that this is only due to packing effects, since no indication for the formation of stable *syn*- or *anti*-conformers was found in solution. As such, the coupling constants for both complexes are in between the expected range for the different conformers.[7] This suggests, that in contrast to the free ligands, which showed both (**1**) or only the *syn*-conformer (**2**) in solution, rapid rotation about the P−C bond takes place in the metal complexes. This can easily be understood, since the conformers are the result of the repulsion between the two lone pairs at the carbon and phosphorus atoms. This repulsion should become decisively smaller upon coordination of the phosphine to the metal and the involvement of the lone pair in the metal bonding.

The η^2 coordination of one of the phenyl groups of the PPh_3 moiety in Y_sPPh_2 to nickel can be viewed as a first step for P−C bond activation and the transfer of the phenyl group to nickel, although no P−C bond elongation was observed. This is in contrast to the observations previously made in the palladium chemistry of other YPhos ligands. Here, YPhos ligands with triphenylphosphonium groups readily reacted with different Pd(0) precursors under P−C bond cleavage.[9] Any attempts to isolate corresponding palladium(0) complexes with Y_sPPh_2 failed. For example, treatment of **1** with Pd_2dba_3 (dba = dibenzylideneacetone) resulted in unselective decomposition reactions, including P−C bond activation. This was

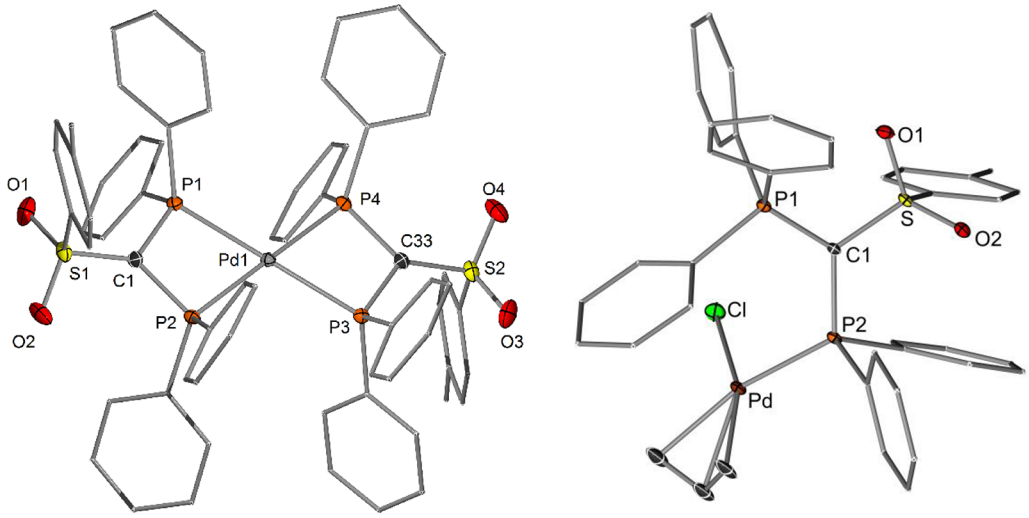

Figure 4. Molecular structures of palladium complexes **3** and $[(\kappa P\text{-}\mathbf{1})Pd(allyl)Cl]$. Hydrogen atoms and solvent molecules are omitted for clarity; only one of the two molecules in the asymmetric unit is shown. Displacement parameters at the 50% level. Selected bond lengths [Å] and angles [deg]: **3**, P(1)−C(1) 1.7517(13), P(2)−C(1) 1.7516(13), S(1)−C(1) 1.7015(13), Pd(1)−P(1) 2.3374(3), Pd(1)−P(2) 2.3257(3), Pd(1)−P(3) 2.3300(3), Pd(1)−P(4) 2.3236(3), P(1)−Pd(1)−P(2) 71.980(11), S(1)−C(1)−P(1) 126.90(8), P(2)−C(1)−P(1) 102.92(7), S(1)−C(1)−P(2) 129.32(8); $[(\kappa P\text{-}\mathbf{1})Pd(allyl)Cl]$, P(1)−C(1) 1.739(4), S(1)−C(1) 1.721(4), C(1)−P(2) 1.782(4), Pd(1)−P(2) 2.3344(11), Cl(1)−Pd(1) 2.3837(11), Pd(1)−C(39A) 2.192(8), Pd(1)−C(40A) 2.149(6), Pd(1)−C(41A) 2.132(9), S(1)−C(1)−P(1) 114.5(2), P(1)−C(1)−P(2) 123.6(2).

DOI: 10.1021/acs.inorgchem.9b00948
Inorg. Chem. 2019, 58, 8151−8161

confirmed by the isolation of small amounts of single crystals of palladium complex **3** with two monoanionic diphosphine ligands (Figure 4). These ligands are formed via cleavage of one of the P−C_{Ph} bonds of the PPh_3 moiety. Presumably, the cleaved phenyl group adds to the dba ligand. However, the mechanism of this transfer is unclear so far. In contrast to the behavior of **1** toward Pd(0) complexes, the reactivity toward Pd(II) complexes was—as expected—more selective. Treatment of the ligand with the Pd(II) precursor $[Pd(allyl)Cl]_2$ selectively gave way to the expected complex [(κ*P*-**1**)Pd(allyl)Cl], which was isolated in 63% yield as an off-white solid. XRD analysis of the complex confirms the simple coordination of the YPhos ligand via the phosphine donor. As expected for the Pd(II) center no additional coordination of one of the phenyl groups is observed, despite the *syn*-arrangement of the Pd(allyl) fragment with the PPh_3 moiety (Figure 4).

The observations made for the group 10 metals led us to further explore the coordination chemistry of Y_SPPh_2 toward group 9 metals. We particularly focused on precursors in the oxidation state I which might lead to further activation reactions or unique coordination behavior. At first the two frequently used rhodium precursors $[Rh(CO)_2Cl]_2$ and $[Rh(COD)Cl]_2$ were tested. Treatment of Y_SPPh_2 with 1 equiv of $[Rh(CO)_2Cl]_2$ led to the selective formation of the new complex [(κ*P*,κ*O*-**1**)Rh(CO)Cl] (Scheme 2), which could

Scheme 2. Preparation of Rhodium Complex [(κ*P*,κ*O*-1)Rh(CO)Cl]

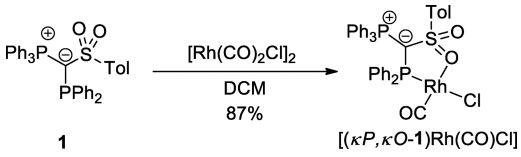

1 [(κ*P*,κ*O*-**1**)Rh(CO)Cl]

be isolated as yellow solid in 87% yield (Figure 5). The $^{31}P\{^1H\}$ NMR spectrum of the product features two sets of

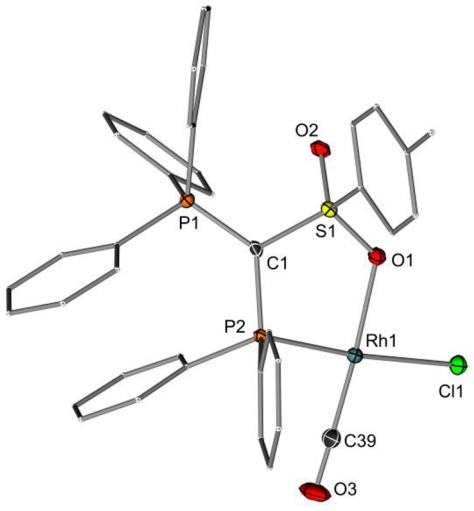

Figure 5. Molecular structure of [(κ*P*,κ*O*-**1**)Rh(CO)Cl]. Hydrogen atoms are omitted for clarity; displacement parameters at the 50% level. Selected bond lengths [Å] and angles [deg]: C(1)−S(1) 1.700(3), C(1)−P(1) 1.725(3), C(1)−P(2) 1.785(3), Rh(1)−P(2) 2.2013(8), Rh(1)−Cl(1) 2.3666(8), Rh(1)−O(1) 2.105(2), Rh(1)−C(39) 1.779(4), O(3)−C(39) 1.144(4), S(1)−C(1)−P(1) 115.52(17), P(1)−C(1)−P(2) 127.84(17).

doublets of doublets due to the coupling of the two phosphorus nuclei with each other and the Rh center. The phosphine signal appears at δ_P = 37.0 ppm and exhibits the expected large coupling constant of $^1J_{PRh}$ = 142.7 Hz. Diffusion of benzene into a solution of [(κ*P*,κ*O*-**1**)Rh(CO)Cl] in chloroform gave single crystals suitable for XRD analysis (monoclinic space group $P2_1$). In the structure, the YPhos ligand acts as a bidentate ligand coordinating to the rhodium center via the phosphine and the sulfonyl group. Thus, coordination of the phosphine to rhodium is accompanied by the release of one CO ligand. The rhodium atom adopts a square-planar geometry with the chloro ligand in *trans*-position to the phosphine donor. The CO stretching frequency of $\tilde{\nu}$ = 1978.6 cm^{-1} as determined by IR spectroscopy is rather low compared to those reported for other phosphine and even carbene ligands.[14] However, due to the coordination of the sulfonyl group to the rhodium center, no correlation with reported TEP values and thus no direct comparison to other monodentate ligands is possible. However, previous IR measurements of the *in situ* formed [(κ*P*-Y_SPPh_2)Rh(acac)-CO] complex already confirmed the high donor capacity of Y_SPPh_2.[7]

Despite the facile preparation of [(κ*P*,κ*O*-**1**)Rh(CO)Cl] the reaction of Y_SPPh_2 with $[Rh(COD)Cl]_2$ was found to be more complex. After mixing of the compounds in THF the formation of two sets of signals with 2:1 intensity was observed by $^{31}P\{^1H\}$ NMR spectroscopy (Figure 6). The minor species **4a** showed two doublets of doublets at δ_P = 20.5 ppm ($^3J_{PRh}$ = 6.5 Hz) and δ_P = 16.9 ppm ($^1J_{PRh}$ = 132.6 Hz). These signals clearly argue for the coordination of the YPhos ligand via the phosphine donor, while the phosphonium moiety remains intact. In contrast, the main species **4b** showed two doublets of doublets with similar $^{31}P\{^1H\}$ NMR shifts (δ_P = 3.7 and 2.8 ppm) and two distinct, large coupling constants between phosphorus and rhodium ($^1J_{PRh}$ = 121.8 and 113.8 Hz) and of the two phosphorus atoms with each other ($^2J_{PP}$ = 41.8 Hz). These NMR features indicate the cleavage of the P−C bond of one of the phosphonium bound phenyl groups and coordination of the ligand to the metal center via two phosphine moieties as already observed for palladium complex **3** (see above). The slightly different NMR shifts of the two phosphorus atoms probably result from a square planar or octahedral geometry of the complex with slightly different environments.

In order to elucidate the structure of the formed compounds, isolation of both species was attempted. However, changing of the reaction conditions (solvent, temperature) always resulted in the same 1:2 ratio between **4a** and **4b**. While **4a** and **4b** could be separated from any other impurity and cleanly isolated, all attempts to separate these species by crystallization or chromatography failed. Addition of further coligands (amines, phosphines) resulted in noticeable changes in the NMR spectra, which however were found to be difficult to explain or to correlate with any possible complex structure. Fortunately, under an ammonia atmosphere, single crystals could be obtained, which revealed the formation of the chloro-bridged dimer **5** (Figure 7). **5** crystallizes as C_i-symmetric complex in the triclinic space group $P\bar{1}$. The molecular structure confirms the P−C bond cleavage and the formation of the anionic bidentate ligand with two PPh_2 donor sites, which we already expected from the reaction mixture (Figure 6). The rhodium atom adopts an octahedral geometry, in which the phenyl and ammonia ligands are perpendicularly

DOI: 10.1021/acs.inorgchem.9b00948
Inorg. Chem. 2019, 58, 8151−8161

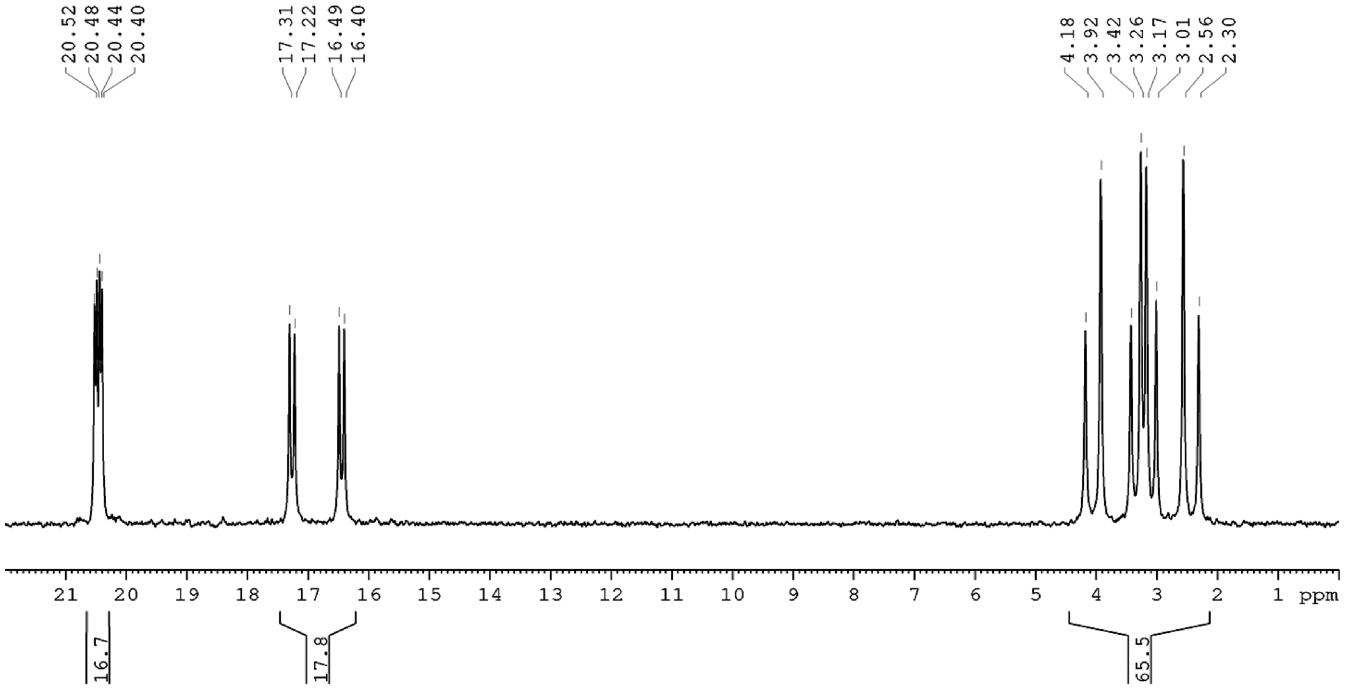

Figure 6. Extract from the $^{31}P\{^{1}H\}$ NMR spectrum of the reaction of Y_SPPh_2 with $[Rh(COD)Cl]_2$.

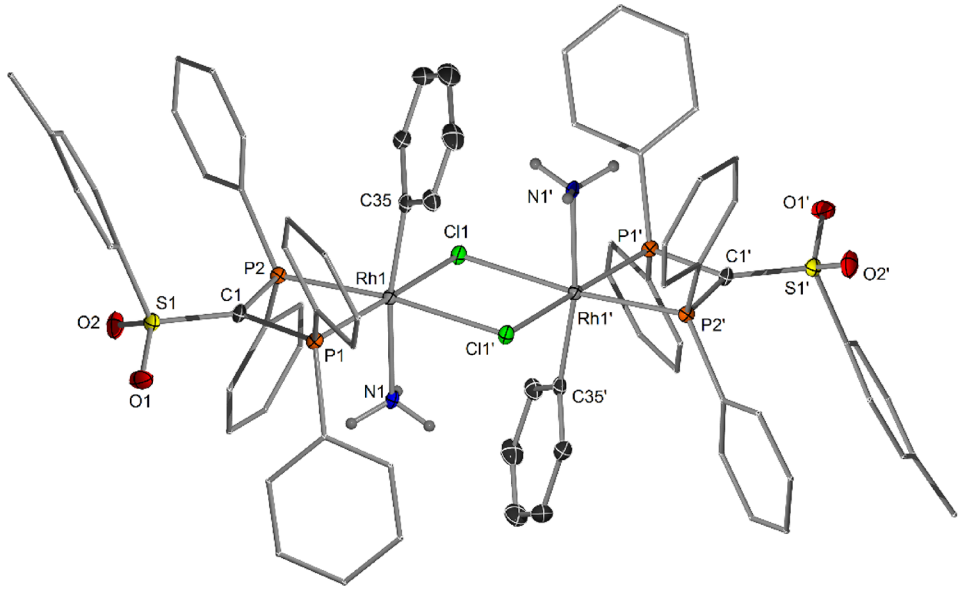

Figure 7. Molecular structure of complex **5**. Hydrogen atoms and solvent molecules are omitted for clarity. Displacement parameters at the 50% level. Selected bond lengths [Å] and angles [deg]: P(1)−C(1) 1.740(2), P(2)−C(1) 1.741(2), S(1)−C(1) 1.695(2), Rh(1)−P(1) 2.2602(6), Rh(1)−P(2) 2.2600(6), Rh(1)−C(35) 2.026(2), Rh(1)−N(1) 2.2222(17), Rh(1)−Cl(1) 2.4603(5), Rh(1)−Cl(1)′ 2.4657(5), P(1)−C(1)−P(2) 99.20(10), S(1)−C(1)−P(1) 133.18(13), S(1)−C(1)−P(2) 127.54(12).

arranged to the plane of the phosphine and chlorido ligands. The P−C distances in the carbanionic ligand of 1.741(2) and 1.740(2) Å are shorter than those found in all other complexes. The central carbon atom features an ideal planar geometry (sum of angles: 359.9(2)°) due to the stabilization of the lone pair via negative hyperconjugation. Complex **5** proofs the proposed P−C activation, which was already expected due to the NMR pattern observed for the reaction of Y_SPPh_2 with $[Rh(COD)Cl]_2$. However, the C_i symmetry of **5** and that of the thus identical PPh_2 moieties disagree with the slightly different shifts observed for the reaction mixture.

Since separation of the two species seen in the NMR spectra (Figure 6) failed, the elucidation of their identity was attempted by their conversion into separable compounds. To this end, $AgBF_4$ was added to a solution of a purified sample of **4a** and **4b** in $CDCl_3$ for halide abstraction. While the addition of the silver salt led to no distinctive changes in the NMR patterns corresponding to the species **4a**, the signals for **4b** changed from the observed two doublet of doublets to a single doublet (δ_P = −15.0 ppm, $^{1}J_{PRh}$ = 101.7 Hz). The isolation of this new species was unsuccessful but provided a valuable hint to the identity of the unknown compound. Since the observed spectrum upon addition of $AgBF_4$ corroborates with a

DOI: 10.1021/acs.inorgchem.9b00948
Inorg. Chem. 2019, 58, 8151−8161

Scheme 3. Reaction of 1 with $[Rh(COD)Cl]_2$

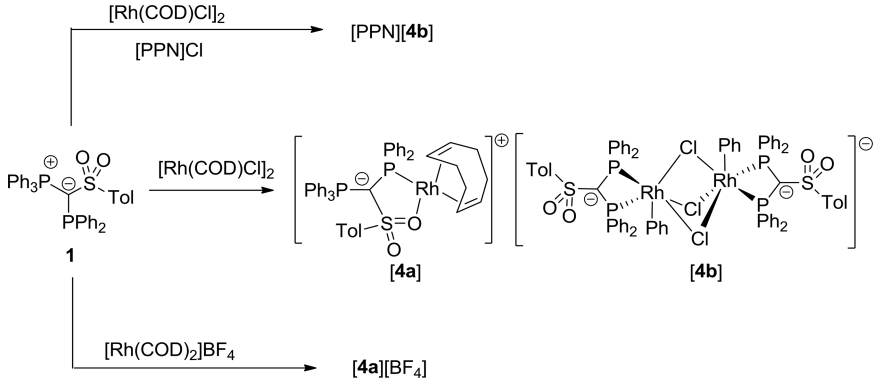

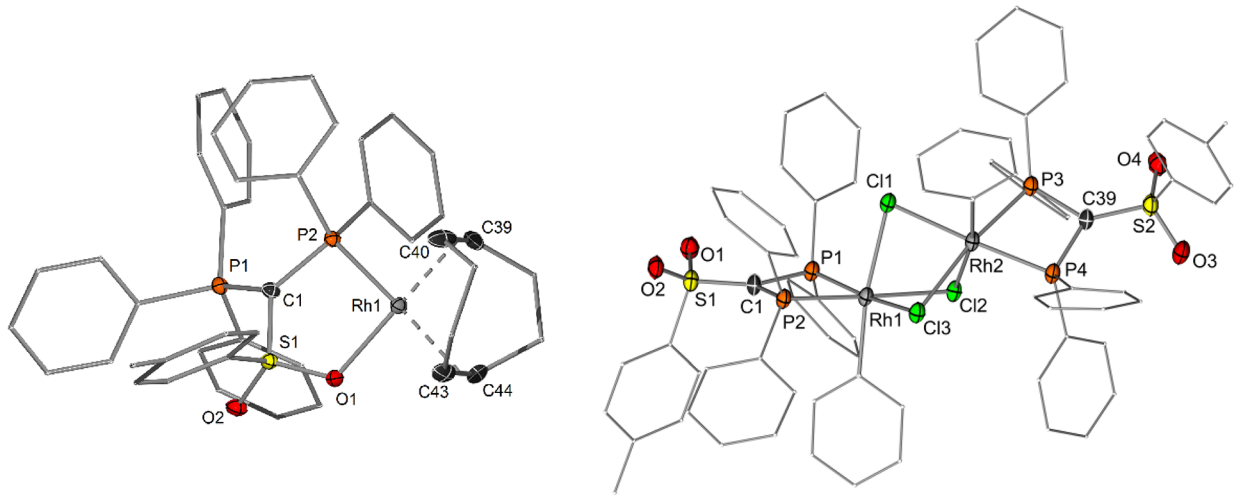

Figure 8. Molecular structures of (left) [**4a**][BF_4] and (right) [PPN][**4b**]. Only the rhodium complexes are shown. The corresponding counterions and solvent molecules are omitted for clarity. Displacement parameters at the 50% level. Selected bond lengths [Å] and angles [deg]: [**4a**][BF_4], P(1)−C(1) 1.7457(14), P(2)−C(1) 1.7809(14), S(1)−C(1) 1.7006(14), Rh(1)−P(2) 2.3052(3), Rh(1)−O(1) 2.1129(10), S(1)−C(1)−P(1) 113.79(8), P(1)−C(1)−P(2) 131.16(8), [PPN][**4b**], P(1)−C(1) 1.771(2), P(2)−C(1) 1.766(2), S(1)−C(1) 1.698(2), Rh(1)−P(1) 2.2518(5), Rh(1)−P(2) 2.2508(5), Rh(1)−C(33) 2.056(2), Rh(1)−Cl(1) 2.5160(5), Rh(1)−Cl(2) 2.5064(5), Rh(1)−Cl(3) 2.4639(5), S(1)−C(1)−P(1) 127.77(14), P(2)−C(1)−P(1) 97.53(11).

spectrum of a symmetrical dinuclear rhodium complex, such as compound **5**, and since it is presumably produced by chloride abstraction, this suggested that the major species **4b** is a dinuclear rhodium complex bridged by three chloride ligands. Because such a complex would be anionic, species **4a** must ultimately be a cationic mononuclear rhodium complex. This ultimately explains the constant 2:1 signal intensity and the fact that the two species could not be separated. To support this conclusion, the independent synthesis of both, the cation **4a** and anion **4b** was attempted (Scheme 3). For isolation of cation **4a**, **1** was reacted with $[Rh(COD)_2]BF_4$, which allowed the isolation of [(κ*P*,κ*O*-**1**)Rh(COD)]BF_4 ([**4a**][BF_4]) in 92% yield. The ^{31}P NMR spectrum of [**4a**][BF_4] exhibits the two doublets at δ_P = 20.5 and δ_P = 16.9 ppm, thus corroborating with the signals observed for the reaction mixture of **1** with $[Rh(COD)Cl]_2$ (Figure 6). Fortunately, the anionic part **4b** of the complex salt could likewise be formed by addition of 0.5 equiv of [PPN]Cl (PPN = bis(triphenylphosphine)iminium) as chloride donor to the reaction of **1** with $[Rh(COD)Cl]_2$, thus giving [PPN][**4b**] as a yellow solid in 64% yield, which could be fully characterized and unambiguously identified by X-ray crystallography (see below). [PPN][**4b**] is a dinuclear rhodium(III) complex bridged by three chloride ligands, in which the two coordinating Y_SPPh_2 ligands underwent P−C bond splitting via formal oxidative addition at rhodium. The NMR data of this complex reflected the signals observed in the original product mixture thus confirming the overall formation of the complex salt [**4a**][**4b**] from the reaction of **1** with $[Rh(COD)Cl]_2$. The ammonia complex **5** obtained from this complex salt by exposure with NH_3 probably results from reaction with the anionic complex $[\mathbf{4b}]^-$ by replacement of one bridging chloride ligand by two NH_3 ligands and formation of [**1**·Rh(COD)]Cl.

The molecular structures of [**4a**][BF_4] and [PPN][**4a**] were both determined by X-ray crystallography. Figure 8 only shows the cationic and anionic rhodium complexes, respectively. In the cationic complex, the rhodium atom features a square-planar geometry with the YPhos ligand coordinating via the phosphine and sulfonyl group similar to [(κ*P*,κ*O*-**1**)Rh(CO)-Cl] (Figure 5). The Rh−P bond amounts to 2.3052(3) Å and is thus longer than in the neutral complex [(κ*P*,κ*O*-**1**)Rh-(CO)Cl]. The Rh(III) centers in **4b** feature a distorted octahedral geometry, with the bridging chlorido ligands adopting one common face of the two octahedra. In contrast to the C_i symmetric ammonia complex **5**, the symmetry in **4b** is broken by the additional chlorido ligand. This results in

DOI: 10.1021/acs.inorgchem.9b00948
Inorg. Chem. 2019, 58, 8151−8161

slightly different environments of the two phosphorus atoms in both ligands, which is thus in line with the slightly different shifts observed in the ^{31}P NMR spectrum. Analogous complexes with a Rh(μ-Cl)$_3$Rh unit were reported with other phosphine or cyclopentadienyl ligands.[15] The Rh−Cl bond to the chlorido ligand (2.549(1) and 2.516(1) Å) in *trans* position to the phenyl ligand is considerable longer than those trans to the phosphine ligand (2.453(1)−2.506(1) Å) due to the different *trans* effect of both ligands. The P−Rh−P angles are rather acute (72.5(1)°) due to the strained diphosphine bite angle. Also, the Cl−Rh−C angles strongly deviate from the ideal linear geometry.

To gain further information about the coordination chemistry of Y_SPPh_2 toward group 9 metals the ligand was treated with half an equivalent of [Ir(COD)Cl]$_2$. In contrast to the rhodium complex, only a single complex was formed, as suggested by NMR spectroscopy, which could be isolated in 78% yield and fully characterized. The complex was identified as complex **6**, in which instead of a P−C bond cleavage an *ortho*-metalation of one phenyl group of the triphenylphosphonium moiety occurred (Scheme 4). The complex shows

Scheme 4. Formation of 6 via Cyclometalation

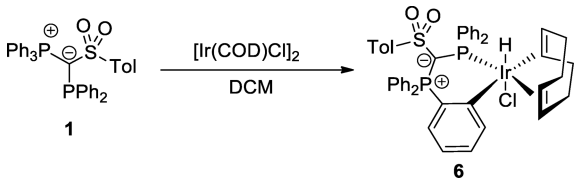

two doublets at δ_P = 27.5 ppm and δ_P = −2.9 ppm in the $^{31}P\{^1H\}$ NMR spectrum ($^2J_{PP}$ = 65.7 Hz). The hydride signal appears as a doublet at δ_H = −15.65 ppm with a coupling constant of $^2J_{HP}$ = 14.4 Hz. Unambiguous confirmation of the *ortho*-metalation was provided by XRD analysis. Single crystals were obtained by diffusion of *n*-hexane into a solution of **6** in THF. The complex crystallizes in the triclinic space group $P\bar{1}$ with two molecules in the asymmetric unit. The hydrido ligand in the complex was directly found in the difference Fourier map and refined independently. In the structure, the iridium center adopts an octahedral geometry (Figure 9). Due to the orthometalation, $\mathbf{Y_SPPh_2}$ acts as monoanionic bidentate ligand, coordinating to the metal via the phosphine and aryl moiety. The phosphine and the COD ligand are *trans* to each other. The Ir−P bond lengths of 2.334(1) and 2.313(1) Å are in the range of reported Ir(III)−P distances.[16] The P1−C1 distance to the phosphonium moiety of 1.743(4) Å is slightly shorter than the one found to the phosphine group (1.779(4) Å), albeit the difference is less pronounced than in the free ligand **1**.[7]

CONCLUSIONS

In conclusion, we reported a detailed investigation of the coordination chemistry of the ylide-functionalized phosphine Y_SPPh_2 toward group 9 and 10 metals using metal precursors often used in transition metal catalysis. The formed complexes demonstrate on the one hand the strong donor properties of the ligand and on the other hand its diverse coordination chemistry. As such, the ligand can act as neutral mono and bidentate ligand binding via the phosphine and sulfonyl group to the metal center. In case of low-valent metal centers (Ni(0), Pd(0), Rh(I), and Ir(I)) bond activation reactions in the

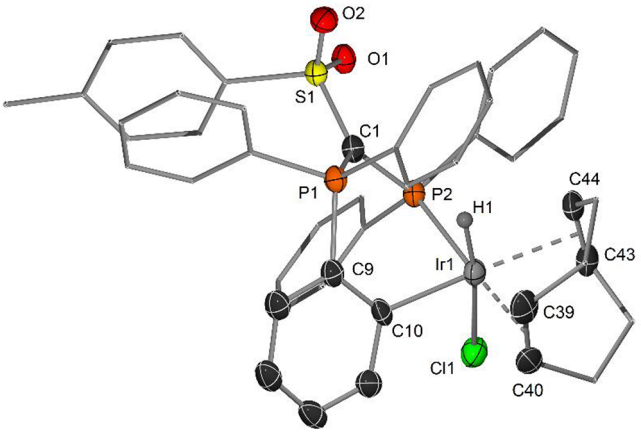

Figure 9. Molecular structure of complex **6•**. Hydrogen atoms and solvent molecules are omitted for clarity; only one of the two molecules in the asymmetric unit is shown. Displacement parameters at the 50% level. Selected bond lengths [Å] and angles [deg]: Ir(1)−C(10) 2.066(3), Ir(1)−Cl(1) 2.4711(10), Ir(1)−P(2) 2.3335(9), Ir(1)−H(1) 1.46(4) P(1)−C(1) 1.743(4), S(1)−C(1) 1.726(4), P(2)−C(1) 1.779(4)

ligand can be observed. This results in either a cleavage (Pd, Rh) or a weakening (Ni) of the P−C bond to one of the phenyl groups of the phosphonium moiety or in an ortho-metalation reaction (Ir). Overall, these findings provide valuable insights into the coordination chemistry of YPhos ligands and give important information for further improvements of the ligand design. The latter will be important for further applications of these ligands in catalysis.

EXPERIMENTAL SECTION

General Procedures. All manipulations were performed under a dry, oxygen-free argon atmosphere in dried Schlenk-type glassware or in an argon-filled glovebox. Involved solvents were dried using an MBraun SPS-800 (THF, Toluene, Et2O, DCM, Pentane, Hexane) or dried in accordance with standard procedures. ^1H, $^{13}C\{^1H\}$, $^{31}P\{^1H\}$ NMR spectra were recorded on Avance I 500 or Avance III 400 spectrometers at 25 °C if not stated otherwise. ^1H and $^{13}C\{^1H\}$ chemical shifts were referenced to the residual ^1H and ^{13}C resonances of the deuterated solvents and are reported relative to TMS. $^{31}P\{^1H\}$ resonances were referenced to external 85% phosphoric acid. All values of the chemical shift are in ppm regarding the δ-scale. All spin−spin coupling constants (J) are printed in hertz (Hz). To display multiplicities and signal forms correctly the following abbreviations were used: s = singlet, d = doublet, t = triplet, m = multiplet, dd = doublet of doublet, dt = doublet of triplet, and br = broad signal. Signal assignment was supported by DEPT, APT, HSQC and HMBC experiments. Elemental analyses were performed on an Elementar vario MICRO cube elemental analyzer. **1**,[17] **2**,[7] **2**·Ni(CO)$_3$,[7] [Rh(COD)Cl]$_2$,[18] Rh(COD)$_2$BF$_4$,[19] and Ni(CO)$_4$[20] were prepared according to published procedures. All other reagents were purchased from Sigma-Aldrich, ABCR, Rockwood Lithium, or Acros Organics and used without further purification.

Synthesis of [1·Ni(CO)$_2$]. **1** (400 mg, 0.65 mmol) was dissolved in 20 mL of benzene and a 0.6 M solution of Ni(CO)$_4$ in benzene (1.6 mL, 0.98 mmol) was added dropwise. For 6 h, the solution was stirred and argon was bubbled through it slowly to remove CO. The solvent was reduced to about 3 mL under vacuum and filtered and then 6 mL of pentane were added, upon which a solid precipitated. The solid was filtered off, and dried under vacuum, The solid was dissolved in 20 mL of a hot 1:1 mixture of toluene and cyclohexane and the stored at 5 °C for several days, upon red crystals of **1**·Ni(CO)$_2$ formed. The crystals were removed from the supernatants and dried, affording crude **1**·Ni(CO)$_2$ (purity was 85%, according to

DOI: 10.1021/acs.inorgchem.9b00948
Inorg. Chem. 2019, 58, 8151−8161

$^{31}P\{^{1}H\}$ NMR) as a red-orange solid. (110 mg, 0.15 mmol, 23%). Single crystals of **1**·Ni(CO)$_2$ suitable for X-ray crystallography were obtained by slow diffusion of pentane into a solution of **1**·Ni(CO)$_2$ in Benzene. Single crystals of **1**·Ni(CO)$_3$ suitable for X-ray crystallography were instead obtained by slow diffusion of pentane into a solution of **1**·Ni(CO)$_2$ in DCM under an atmosphere of CO. ^{1}H NMR (400.3 MHz, CD_2Cl_2, −30 °C): δ = 1.83 (s, 3H; CH_3), 6.42−6.54 (m, 4H; CH_{Tol}), 6.80−7.18 (m, 20H; CH_{PPh}), 7.20−7.27 (m, 4H; CH_{PPh}), 7.43−7.52 (m, 6H; CH_{PPh}), 8.32−8.41 (m, 29H; CH_{PPh}). $^{31}P\{^{1}H\}$ NMR (162.1 MHz, CD_2Cl_2, −30 °C): δ = 24.8.

Isolation of Crystals of 3. **1** (20 mg, 32.5 μmol) and Pd(dba)$_2$ (19 mg, 33.0 mmol) were dissolved in 0.6 mL of THF-d_8. The solution was heated to 60 °C for 16 h and then filtered. Slow evaporation of the solution lead to the formation of orange crystals of **3**, suitable for X-ray crystallography.

Synthesis of [(κ*P*-1)Pd(allyl)Cl]. **1** (201 mg, 0.325 mmol) and [PdCl(η^3-C_3H_5)]$_2$ (59 mg, 0.163 mmol) were dissolved in 10 mL of DCM and stirred for 1 h. The solvent was reduced to about 5 mL under vacuum, and then 10 mL of pentane was added, upon which a solid precipitated. The solid was filtered off, washed with 5 mL of pentane, and dried under vacuum, affording **1**·Pd(allyl)Cl as an off-white solid (163 mg, 0.21 mmol, 63%). Single crystals suitable for X-ray crystallography were obtained by slow diffusion of pentane into a solution of **1**·Pd(allyl)Cl in DCM. ^{1}H NMR (500.1 MHz, CD_2Cl_2): δ = 1.8−2.5 (br, 2H; $CH_{2,\ allyl}$), 2.22 (s, 3H; CH_3), 2.76 (br, 1H; $CH_{2,\ allyl}$), 4.12 (m, 1H; $CH_{2,\ allyl}$), 4.84 (br, 1H; CH_{allyl}), 6.71−6.73 (m, 2H; $CH_{Tol,\ meta}$), 6.76−6.78 (m, 2H; $CH_{Tol,\ ortho}$), 7.16−7.18 (m, 4H; $CH_{PdPPh,\ meta}$), 7.22−7.25 (m, 2H; $CH_{PdPPh,\ para}$), 7.41−7.45 (m, 6 H; $CH_{PPh,\ meta}$), 7.53−7.57 (m, 3H; $CH_{PPh,\ para}$), 7.84−7.88 (m, 4H; $CH_{PdPPh,\ ortho}$), 7.97−8.01 (m, 6H; $CH_{PPh,\ ortho}$). $^{13}C\{^{1}H\}$ NMR (125.8 MHz, CD_2Cl_2): δ = 21.3 (CH_3), 42.3 (dd, $^{1}J_{CP}$ = 105.2 Hz, $^{1}J_{CP}$ = 20.4 Hz; C_{PCS}), 64.7 (br; $CH_{2,\ allyl}$), 78.3 (d, $^{2}J_{CP}$ = 31.8 Hz; $CH_{2,\ allyl}$), 117.7 (d, $^{2}J_{CP}$ = 4.3 Hz; CH_{allyl}), 126.5 ($CH_{Tol,\ ortho}$), 127.4 (d, $^{2}J_{CP}$ = 10.3 Hz; $CH_{PdPPh,\ meta}$), 128.3 (dd, $^{1}J_{CP}$ = 94.0 Hz, $^{3}J_{CP}$ = 1.2 Hz; $C_{PPh,\ ipso}$), 128.4 (dd, $^{1}J_{CP}$ = 55.1 Hz, $^{3}J_{CP}$ = 12.4 Hz; $CH_{PdPPh,\ ipso}$), 128.5 ($CH_{Tol,\ meta}$), 128.5 (d, $^{3}J_{CP}$ = 12.8 Hz; $CH_{PPh,\ meta}$), 129.4 (d, $^{4}J_{CP}$ = 2.0 Hz; $CH_{PdPPh,\ para}$), 132.3 (d, $^{4}J_{CP}$ = 3.0 Hz; $CH_{PPh,\ para}$), 135.2 (d, $^{2}J_{CP}$ = 10.5 Hz; $CH_{PdPPh,\ ortho}$), 136.2 (d, $^{2}J_{CP}$ = 10.1 Hz; $CH_{PPh,\ ortho}$), 140.9 ($C_{Tol,\ para}$), 144.2 ($C_{Tol,\ ipso}$). $^{31}P\{^{1}H\}$ NMR (162.0 MHz, CD_2Cl_2): δ = 9.9 (d, $^{2}J_{PP}$ = 67.3 Hz), 22.9 (d, $^{2}J_{PP}$ = 67.3 Hz). Anal. Calcd for $C_{41}H_{37}O_2P_2SClPd$: C, 61.74; H 4.68; S, 4.02. Found: C, 61.47; H 4.69; S, 3.72

Synthesis of [(κ*P*,κ*O*-1)Rh(CO)Cl]. **1** (500 mg, 0.81 mmol) and [Rh(CO)$_2$Cl]$_2$ (158 mg, 0.41 mmol) were dissolved in 15 mL of DCM, which resulted in vigorous gas evolution. The solution was stirred for 30 min, and was filtered to remove a small amount of insoluble material. Under stirring, 15 mL of pentane was added, which resulted in the formation of a yellow precipitate. The solid was filtered off, washed twice with 5 mL of pentane and dried under vacuum, affording **1**·Rh(CO)Cl as a yellow solid (553 mg, 0.71 mmol, 87%). Single crystals suitable for X-ray crystallography were obtained by slow diffusion of benzene into a solution of **1**·Rh(CO)Cl in chloroform. ^{1}H NMR (500.1 MHz, CD_2Cl_2): δ = 2.38 (s, 3H; CH_3), 6.92−6.98 (m, 2H; $CH_{RhPPh,\ meta}$), 6.99−7.03 (m, 2H; $CH_{Tol,\ meta}$), 7.11−7.16 (m, 1H; $CH_{RhPPh,\ para}$), 7.22−7.25 (m, 2H; $CH_{Tol,\ ortho}$), 7.32−7.43 (m, 12H; $CH_{PPh,\ ortho+RhPPh,\ ortho+RhPPh,\ meta}$), 7.43−7.54 (m, 7H; $CH_{PPh,\ ortho+RhPPh,\ para}$), 7.57−7.62 (m, 3H; $CH_{PPh,\ para}$). $^{13}C\{^{1}H\}$ NMR (125.8 MHz, CD_2Cl_2): δ = 21.6 (CH_3), 41.6 (dd, $^{1}J_{CP}$ = 91.4 Hz, $^{1}J_{CP}$ = 33.8 Hz; C_{PCS}), 122.8 (d, $^{1}J_{CP}$ = 92.6 Hz; $C_{PPh,\ ipso}$), 126.7 ($CH_{Tol,\ ortho}$), 128.1 (d, $^{3}J_{CP}$ = 11.9 Hz; $CH_{RhPPh,\ meta}$), 128.7 (d, $^{3}J_{CP}$ = 11.3 Hz; $CH_{RhPPh,\ meta}$), 129.1 (d, $^{3}J_{CP}$ = 12.7 Hz; $C_{PPh,\ meta}$), 129.4 ($CH_{Tol,\ meta}$), 130.4 (d, $^{4}J_{CP}$ = 2.5 Hz; $CH_{RhPPh,\ para}$), 130.5 (d, $^{4}J_{CP}$ = 2.5 Hz; $CH_{RhPPh,\ para}$), 131.9 (d, $^{2}J_{CP}$ = 12.3 Hz; $CH_{RhPPh,\ ortho}$), 132.2 (d, $^{1}J_{CP}$ = 58.0 Hz; $C_{RhPPh,\ ipso}$), 133.6 (d, $^{4}J_{CP}$ = 2.9 Hz; $CH_{PPh,\ para}$), 133.9 (d, $^{1}J_{CP}$ = 58.3 Hz; $C_{RhPPh,\ ipso}$), 135.0 (d, $^{2}J_{CP}$ = 14.0 Hz; $CH_{RhPPh,\ ortho}$), 135.4 (d, $^{2}J_{CP}$ = 10.3 Hz; $CH_{PPh,\ ortho}$), 142.0 ($C_{Tol,\ para}$), 143.4 ($CH_{Tol,\ ipso}$), 188.0 (dd, $^{1}J_{CRh}$ = 85.1 Hz, $^{2}J_{CP}$ = 15.6 Hz; C_{RhCO}). $^{31}P\{^{1}H\}$ NMR (202.5 MHz, CD_2Cl_2): δ = 19.3 (dd, $^{2}J_{PP}$ = 9.5 Hz, $^{3}J_{PRh}$ = 7.8 Hz), 37.0 (dd, $^{1}J_{PRh}$ = 142.7 Hz, $^{2}J_{PP}$ = 9.5 Hz). Anal. Calcd for $C_{39}H_{32}O_3P_2SClRh$: C, 59.97; H 4.13; S, 4.10. Found: C, 59.93; H 4.12; S, 3.89.

Synthesis of [4a][BF4]. **1** (306 mg, 0.50 mmol) and Rh(COD)$_2$BF$_4$ (200 mg, 0.50 mmol) were dissolved in 3 mL of THF and stirred for 1 h, during which a yellow solid precipitated. To the mixture was added 2 mL of Et$_2$O, and the mixture was stirred for another 30 min. The solid was filtered off and washed twice with 2 mL of Et$_2$O and dried under vacuum, affording [**4a**][BF$_4$] as a yellow solid (410 mg, 0.45 mmol, 92%). NMR spectra of this compound were recorded at −30 °C, since some signals were very broad at room temperature. Single crystals suitable for X-ray crystallography were obtained by slow diffusion of hexane into a solution of [**4a**][BF$_4$] in chloroform. ^{1}H NMR (400.3 MHz, CD_2Cl_2, −30 °C): δ = 1.69−1.83 (m, 1H; $CH_{2,COD}$), 1.83−1.98 (m, 1H; $CH_{2,COD}$), 1.98−2.12 (m, 1H; $CH_{2,COD}$), 2.12−2.39 (m, 3H; $CH_{2,COD}$), 2.39−2.60 (m, 2H; $CH_{2,COD}$), 2.47 (s, 3H; CH_3), 2.71−2.83 (m, 1H; CH_{COD}), 3.17−3.28 (m, 1H; CH_{COD}), 5.18−5.31 (m, 1H; CH_{COD}), 5.44−5.55 (m, 1H; CH_{COD}), 7.10−7.66 (m, 29H; CH). $^{13}C\{^{1}H\}$ NMR (100.7 MHz, CD_2Cl_2, −30 °C): δ = 21.5 (CH_3), 26.4 ($CH_{2,COD}$), 29.5 ($CH_{2,COD}$), 30.5 ($CH_{2,COD}$), 34.0 ($CH_{2,COD}$), 40.0 (dd, $^{1}J_{CP}$ = 88.8 Hz, $^{1}J_{CP}$ = 33.8 Hz; C_{PCS}), 71.7 (d, $^{1}J_{CRh}$ = 14.5 Hz; CH_{COD}), 74.7 (d, $^{1}J_{CRh}$ = 15.4 Hz; CH_{COD}), 104.3 (dd, $^{1}J_{CRh}$ = 10.5 Hz, $^{2}J_{CP}$ = 7.0 Hz; CH_{COD}), 104.3 (dd, $^{1}J_{CRh}$ = 10.7 Hz, $^{2}J_{CP}$ = 6.9 Hz; CH_{COD}), 120.6 (d, $^{1}J_{CP}$ = 92.8 Hz; $C_{PPh,\ ipso}$), 125.5 ($CH_{Tol,\ ortho}$), 128.5 (d, $^{3}J_{CP}$ = 11.5 Hz; $CH_{RhPPh,\ meta}$), 128.6 (d, $^{1}J_{CP}$ = 58.0 Hz; $C_{RhPPh,\ ipso}$), 128.7 (d, $^{3}J_{CP}$ = 12.6 Hz; $C_{PPh,\ meta}$), 129.0 (d, $^{3}J_{CP}$ = 10.8 Hz; $CH_{RhPPh,\ meta}$), 129.3 (d, $^{1}J_{CP}$ = 53.3 Hz; $C_{RhPPh,\ ipso}$), 129.5 ($CH_{Tol,\ meta}$), 130.1 (d, $^{2}J_{CP}$ = 11.0 Hz; $CH_{RhPPh,\ ortho}$), 130.7 ($CH_{RhPPh,\ para}$), 131.3 ($CH_{RhPPh,\ para}$), 133.6 (d, $^{4}J_{CP}$ = 2.2 Hz; $CH_{PPh,\ para}$), 134.7 (d, $^{2}J_{CP}$ = 14.1 Hz; $CH_{RhPPh,\ ortho}$), 134.8 (d, $^{2}J_{CP}$ = 9.7 Hz; $CH_{PPh,\ ortho}$), 141.0 ($C_{Tol,\ para}$), 143.8 ($CH_{Tol,\ ipso}$). $^{31}P\{^{1}H\}$ NMR (162.1 MHz, CD_2Cl_2, −30 °C): δ = 16.6 (dd, $^{1}J_{PRh}$ = 132.2 Hz, $^{2}J_{PP}$ = 13.1 Hz), 20.0 (dd, $^{2}J_{PP}$ = 13.1 Hz, $^{3}J_{PRh}$ = 7.3 Hz). Anal. Calcd for $C_{46}H_{44}BO_2F_4P_2SRh$: C, 60.54; H 4.86; S, 3.51. Found: C, 60.55; H 5.09; S, 3.30.

Synthesis of [PPN][4b]. **1** (600 mg, 0.98 mmol), [Rh(COD)Cl]$_2$ (240 mg, 0.49 mmol), and [PPN]Cl (280 mg, 49 mmol) were dissolved in 30 mL of THF and heated to 55 °C for 3 days, during which a solid precipitated. The solid was filtered off and washed with 10 mL of THF and dried under vacuum. The solid was dissolved in 12 mL of DCM, filtered to remove a small amount of insoluble material, and then precipitated by addition of 12 mL of Et$_2$O. The solid was filtered off and washed twice with 5 mL of Et$_2$O and dried under vacuum, affording [PPN][**4b**] as a yellow solid (795 mg, 0.38 mmol, 64%). Single crystals suitable for X-ray crystallography were obtained by evaporation of a solution of [PPN][**4b**] in a 1:1 DCM:benzene mixture. ^{1}H NMR (400.3 MHz, CD_2Cl_2): δ = 2.20 (s, 6H; CH_3), 6.00−6.09 (m, 4H; $CH_{RhPh,\ meta}$), 6.34−6.42 (m, 2H; $CH_{RhPh,\ para}$), 6.72−6.79 (m, 4H; $CH_{PPh,meta}$), 6.81−6.86 (m, 4H; $CH_{Tol,\ ortho}$), 6.87−6.94 (m, 4H; $CH_{PPh,meta}$), 6.94−6.99 (m, 2H; $CH_{PPh,para,}$), 7.05−7.11 (m, 2H; $CH_{PPh,para,}$), 7.13−7.23 (m, 10H; $CH_{RhPh,ortho}$ + $CH_{PPh,meta}$ + $CH_{PPh,para,}$), 7.32−7.38 (m, 4H; $CH_{Tol,\ meta}$), 7.38−7.55 (m, 34H; $CH_{PPN,ortho}$ + $CH_{PPN,meta}$ + $CH_{PPh,ortho}$ + $CH_{PPh,meta}$ + $CH_{PPh,para,}$), 7.62−7.68 (m, 6H; $CH_{PPN,para,}$), 7.71−7.79 (m, 4H; $CH_{PPh,ortho}$), 7.79−7.86 (m, 4H; $CH_{PPh,ortho}$), 8.15−8.23 (m, 4H; $CH_{PPh,ortho}$). $^{13}C\{^{1}H\}$ NMR (100.7 MHz, CD_2Cl_2): δ = 21.3 (CH_3), 50.6 (dt, $^{1}J_{CP}$ = 42.0 Hz, $^{1}J_{CP}$ = 33.8 Hz; C_{PCS}), 121.8 ($CH_{RhPh,\ para}$), 124.4 ($CH_{RhPh,\ meta}$), 126.6 (d, $^{2}J_{CP}$ = 11.3 Hz; $CH_{PPh,\ ortho}$), 126.7 (d, $^{2}J_{CP}$ = 11.4 Hz; $CH_{PPh,\ ortho}$), 126.8 ($CH_{Tol,\ ortho}$), 127.1 (d, $^{2}J_{CP}$ = 12.1 Hz; $CH_{PPh,\ ortho}$), 127.3 (d, $^{2}J_{CP}$ = 11.9 Hz; $CH_{PPh,\ ortho}$), 127.4 (dd, $^{1}J_{CP}$ = 108.0 Hz, $^{3}J_{CP}$ = 1.9 Hz; $CH_{PPN,ipso}$), 128.6 ($CH_{Tol,\ meta}$), 128.8 (d, $^{4}J_{CP}$ = 2.8 Hz; $CH_{PPh,\ para}$), 129.2 (d, $^{4}J_{CP}$ = 2.2 Hz; $CH_{PPh,\ para}$), 129.3 (d, $^{4}J_{CP}$ = 3.0 Hz; $CH_{PPh,\ para}$), 129.5 (d, $^{4}J_{CP}$ = 2.2 Hz; $CH_{PPh,\ para}$), 129.8−130.0 (m; $CH_{PPN,ortho}$), 132.4−132.6 (m; $CH_{PPN,meta}$), 133.2 (dd, $^{1}J_{CP}$ = 55.5 Hz, $^{3}J_{CP}$ = 3.0 Hz; $C_{PPh,\ ipso}$), 133.3 (dd, $^{1}J_{CP}$ = 56.5 Hz, $^{3}J_{CP}$ = 2.9 Hz; $C_{PPh,\ ipso}$), 134.1 (d, $^{3}J_{CP}$ = 10.8 Hz; $CH_{PPh,\ meta}$), 134.2 ($CH_{PPN,\ para}$), 134.3 (d, $^{3}J_{CP}$ = 10.5 Hz; $CH_{PPh,\ meta}$), 135.7 (d, $^{3}J_{CP}$ = 10.2 Hz; $CH_{PPh,\ meta}$), 136.5 (d, $^{3}J_{CP}$ = 9.8 Hz; $CH_{PPh,\ meta}$), 137.3 (d, $^{1}J_{CP}$ = 59.4 Hz; $C_{PPh,\ ipso}$), 138.6 (d, $^{1}J_{CP}$ = 59.1 Hz; $C_{PPh,\ ipso}$), 141.0 ($C_{Tol,\ para}$), 141.9 ($CH_{RhPh,\ ortho}$),

DOI: 10.1021/acs.inorgchem.9b00948
Inorg. Chem. 2019, 58, 8151−8161

143.8 ($CH_{Tol,\ ipso}$), 146.5 (dt, $^{1}J_{CRh}$ = 30.8 Hz, $^{2}J_{CP}$ = 8.6 Hz $CH_{RhPh,\ ipso}$). $^{31}P\{^{1}H\}$ NMR (162.1 MHz, CD_2Cl_2): δ = 21.0, 3.4 (dd, $^{1}J_{PRh}$ = 121.2 Hz, $^{2}J_{PP}$ = 41.0 Hz), 2.2 (dd, $^{1}J_{PRh}$ = 113.3 Hz, $^{2}J_{PP}$ = 41.0 Hz). Anal. Calcd for $C_{112}H_{94}NO_4P_6S_2Rh_2$: C, 64.67; H 4.56; N, 0.67; S, 3.08. Found: C, 64.69; H 4.54; N, 0.77; S, 2.93.

Synthesis of [4a][4b]. **1** (500 mg, 0.81 mmol) and [Rh(COD)-Cl]$_2$ (200 mg, 0.41 mmol dissolved in 20 mL of THF and heated to 55 °C for 3 days. The solvent was removed under vacuum and the residue was subjected to column chromatography (SiO_2), with a gradient from 50% Ethyl acetate in DCM to 95% ethyl acetate in DCM, affording [**4a**][**4b**] as a pale orange solid (283 mg, 0.12 mmol, 44%). Some signals in the $^{13}C\{^{1}H\}$ NMR spectra for the cationic part (**4a**) are very broad at room temperature and could not be assigned; see synthesis of [**4a**][BF_4]. Single crystals of **5** suitable for X-ray crystallography were obtained by storing a solution of [**4a**][**4b**] in chloroform under an atmosphere of ammonia for several days. ^{1}H NMR (400.3 MHz, CD_2Cl_2): δ = 1.87−2.55 (m, 8H; $CH_{2,COD,\ a}$), 2.20 (s, 6H; $CH_{3,\ b}$), 2.49 (s, 3H; $CH_{3,\ a}$), 2.88−3.24 (m, 2H; CH_{COD}), 5.26−5.50 (m, 2H; CH_{COD}), 6.00−6.09 (m, 4H; $CH_{RhPh,\ meta,\ b}$), 6.34−6.42 (m, 2H; $CH_{RhPh,\ para,\ b}$), 6.72−6.79 (m, 4H; $CH_{PPh,meta,\ b}$), 6.81−6.86 (m, 4H; $CH_{Tol,\ ortho,\ b}$), 6.87−6.94 (m, 4H; $CH_{PPh,meta,\ b}$), 6.94−6.99 (m, 2H; $CH_{PPh,para,\ b}$), 7.05−7.11 (m, 2H; $CH_{PPh,para,\ b}$), 7.13−7.26 (m, 12H; $CH_{RhPh,ortho,\ b}$ + $CH_{PPh,meta,\ b}$ + $CH_{PPh,para,\ b}$+ $CH_{Tol,ortho,\ a}$), 7.27−7.61 (m, 39H; $CH_{PPh,ortho,\ b}$ + $CH_{PPh,meta,\ b}$ + $CH_{PPh,para,\ b}$ + $CH_{Tol,\ meta,\ b}$ + $CH_{PPh,\ a}$+ $CH_{RhPPh,\ a}$), 7.68−7.79 (m, 6H; $CH_{PPh,\ ortho,\ b}$ + $CH_{Tol,meta,\ a}$), 7.79−7.86 (m, 4H; $CH_{PPh,ortho,\ b}$), 8.15−8.23 (m, 4H; $CH_{PPh,ortho,\ b}$). $^{13}C\{^{1}H\}$ NMR (100.7 MHz, CD_2Cl_2): δ = 21.3 ($CH_{3,\ b}$), 21.8 ($CH_{3,\ a}$), 28.5 (br, $CH_{2,COD,\ a}$), 32.7 (br, $CH_{2,COD,\ a}$), 41.1 (dd, $^{1}J_{CP}$ = 88.3 Hz, $^{1}J_{CP}$ = 33.8 Hz; $C_{PCS,\ a}$), 50.6 (dt, $^{1}J_{CP}$ = 42.0 Hz, $^{1}J_{CP}$ = 33.8 Hz; $C_{PCS,\ b}$), 73.5 (br; $CH_{COD,\ a}$), 105.2 (br; $CH_{COD,\ a}$), 121.6 (d, $^{1}J_{CP}$ = 92.2 Hz; $C_{PPh,\ ipso,\ a}$), 121.8 ($CH_{RhPh,\ para,\ b}$), 124.4 ($CH_{RhPh,\ meta,\ b}$), 126.2 ($CH_{Tol,\ ortho,\ a}$), 126.6 (d, $^{2}J_{CP}$ = 11.3 Hz; $CH_{PPh,\ ortho,\ b}$), 126.7 (d, $^{2}J_{CP}$ = 11.4 Hz; $CH_{PPh,\ ortho,\ b}$), 126.8 ($CH_{Tol,\ ortho,\ b}$), 127.1 (d, $^{2}J_{CP}$ = 12.1 Hz; $CH_{PPh,\ ortho,\ b}$), 127.3 (d, $^{2}J_{CP}$ = 11.9 Hz; $CH_{PPh,\ ortho,\ b}$), 128.6 ($CH_{Tol,\ meta,\ b}$), 128.8 (d, $^{4}J_{CP}$ = 2.8 Hz; $CH_{PPh,\ para,\ b}$), 129.17 (d, $^{4}J_{CP}$ = 2.2 Hz; $CH_{PPh,\ para,\ b}$), 129.19 (d, $^{3}J_{CP}$ = 13.0 Hz; $C_{PPh,\ meta,\ a}$), 129.3 (d, $^{4}J_{CP}$ = 3.0 Hz; $CH_{PPh,\ para,\ b}$), 129.5 (d, $^{4}J_{CP}$ = 2.2 Hz; $CH_{PPh,\ para,\ b}$), 129.9 ($CH_{Tol,\ meta,\ a}$), 131.5 ($CH_{RhPPh,\ para,\ a}$), 133.2 (dd, $^{1}J_{CP}$ = 55.5 Hz, $^{3}J_{CP}$ = 3.0 Hz; $C_{PPh,\ ipso,\ b}$), 133.3 (dd, $^{1}J_{CP}$ = 56.5 Hz, $^{3}J_{CP}$ = 2.9 Hz; $C_{PPh,\ ipso,\ b}$), 134.0 (d, $^{4}J_{CP}$ = 3.0 Hz; $CH_{PPh,\ para,\ a}$), 134.1 (d, $^{3}J_{CP}$ = 10.8 Hz; $CH_{PPh,\ meta,\ b}$), 134.3 (d, $^{3}J_{CP}$ = 10.5 Hz; $CH_{PPh,\ meta,\ b}$), 135.3 (d, $^{2}J_{CP}$ = 10.5 Hz; $CH_{PPh,\ ortho,\ a}$), 135.7 (d, $^{3}J_{CP}$ = 10.2 Hz; $CH_{PPh,\ meta,\ b}$), 136.5 (d, $^{3}J_{CP}$ = 9.8 Hz; $CH_{PPh,\ meta,\ b}$), 137.3 (d, $^{1}J_{CP}$ = 59.4 Hz; $C_{PPh,\ ipso,\ b}$), 138.6 (d, $^{1}J_{CP}$ = 59.1 Hz; $C_{PPh,\ ipso,\ b}$), 141.0 ($C_{Tol,\ para,\ b}$), 141.9 ($CH_{RhPh,\ ortho,\ b}$), 142.0 ($C_{Tol,\ para,\ a}$), 143.8 ($CH_{Tol,\ ipso,\ b}$), 144.3 ($CH_{Tol,\ ipso,\ a}$), 146.5 (dt, $^{1}J_{CRh}$ = 30.8 Hz, $^{2}J_{CP}$ = 8.6 Hz $CH_{RhPh,\ ipso,\ b}$). $^{31}P\{^{1}H\}$ NMR (162.1 MHz, CD_2Cl_2): δ = 3.4 (dd, $^{1}J_{PRh}$ = 122.1 Hz, $^{2}J_{PP}$ = 41.8 Hz), 2.2 (dd, $^{1}J_{PRh}$ = 113.6 Hz, $^{2}J_{PP}$ = 41.8 Hz), 16.6 (dd, $^{1}J_{PRh}$ = 132.3 Hz, $^{2}J_{PP}$ = 13.6 Hz), 20.0 (dd, $^{2}J_{PP}$ = 13.6 Hz, $^{3}J_{PRh}$ = 7.6 Hz). Anal. Calcd for $C_{122}H_{108}O_6P_6S_3Cl_3Rh_3$: C, 61.90; H 4.60; S, 4.06. Found: C, 61.68; H 4.60; S, 3.99.

Synthesis of 6. One (400 mg, 0.65 mmol) and [Ir(COD)Cl]2 (220 mg, 0.33 mmol) were dissolved in 20 mL of benzene and stirred for 3 days. The solution was filtered and the remaining solids washed with 2 mL of benzene. The solution was reduced to 10 mL under vacuum, and then 10 mL of pentane was added, which caused precipitation of a solid. The solid was filtered off and washed twice with 5 mL of pentane and dried under vacuum, affording **6** as an off-white solid (486 mg, 0.51 mmol, 78%). NMR spectra of this compound were recorded at −30 °C, since some signals were very broad at room temperature. Single crystals suitable for X-ray crystallography were obtained by slow diffusion of hexane into a solution of **6** in THF. ^{1}H NMR (400.3 MHz, CD_2Cl_2, −30 °C): δ = −15.65 (d, $^{2}J_{HP}$ = 14.4 Hz; *H*Ir) 0.47−0.62 (m, 1H; $CH_{2,COD}$), 1.05−1.19 (m, 1H; $CH_{2,COD}$), 1.38−1.51 (m, 1H; $CH_{2,COD}$), 1.83−2.01 (m, 2H; $CH_{2,COD}$), 2.01−2.14 (m, 1H; $CH_{2,COD}$), 2.13 (s, 3H; CH_3), 2.60−2.84 (m, 2H; $CH_{2,COD}$), 3.23−3.34 (m, 1H; CH_{COD}), 3.51−3.61 (m, 1H; CH_{COD}), 3.84−3.94 (m, 1H; CH_{COD}), 4.21−4.32 (m, 1H; CH_{COD}), 5.47−5.62 (m, 2H; $CH_{Tol,\ ortho}$), 6.20−6.36 (m, 2H; CH_{PPh}), 6.38−6.48 (m, 2H; $CH_{Tol,\ meta}$), 6.83−6.99 (m, 3H; CH_{PPh}), 7.15−7.71 (m, 14H; CH_{PPh}), 7.72−7.81 (m, 1H; CH_{PPh}), 7.94−8.01 (m, 1H; CH_{PPh}), 8.30−8.37 (m, 1H; CH_{PPh}), 8.45−8.57 (m, 1H; CH_{PPh}), 9.34−9.43 (m, 1H; CH_{PPh}). $^{13}C\{^{1}H\}$ NMR (100.7 MHz, CD_2Cl_2, −30 °C): δ = 20.9 (CH_3), 28.0 ($CH_{2,COD}$), 28.8 ($CH_{2,COD}$), 29.0 (d, $^{3}J_{CP}$ = 2.9 Hz $CH_{2,COD}$), 33.0 ($CH_{2,COD}$), 41.5 (dd, $^{1}J_{CP}$ = 111.1 Hz, $^{1}J_{CP}$ = 58.3 Hz; C_{PCS}), 93.2 (d, $^{2}J_{CP}$ = 9.3 Hz; CH_{COD}), 95.2 (CH_{COD}), 97.7 (CH_{COD}), 98.6 (d, $^{2}J_{CP}$ = 17.6 Hz; CH_{COD}), 121.5 (d, J_{CP} = 13.4 Hz; CH_{PPh}), 121.8 (dd, $^{1}J_{CP}$ = 88.2 Hz, $^{3}J_{CP}$ = 8.0 Hz; C_{PPh}), 124.3 ($CH_{Tol,\ ortho}$), 125.4 (d, J_{CP} = 11.6 Hz; CH_{PPh}), 126.1 (d, J_{CP} = 12.5 Hz; CH_{PPh}), 126.5 (d, J_{CP} = 8.5 Hz; CH_{PPh}), 127.1 (d, J_{CP} = 11.1 Hz; CH_{PPh}), 127.7 (d, J_{CP} = 12.0 Hz; CH_{PPh}), 128.3 ($CH_{Tol,\ meta}$), 129.0 (d, J_{CP} = 1.5 Hz; CH_{PPh}), 129.4 (d, J_{CP} = 13.0 Hz; CH_{PPh}), 129.7 (d, J_{CP} = 2.5 Hz; CH_{PPh}), 129.9 (d, J_{CP} = 12.6 Hz; CH_{PPh}), 130.2 (d, $^{1}J_{CP}$ = 86.6 Hz; C_{PPh}), 130.9 (d, J_{CP} = 2.7 Hz; CH_{PPh}), 131.1 (d, J_{CP} = 12.5 Hz; CH_{PPh}), 131.6 (d, J_{CP} = 3.7 Hz; CH_{PPh}), 131.9 (d, J_{CP} = 14.0 Hz; CH_{PPh}), 132.4 (d, J_{CP} = 2.6 Hz; CH_{PPh}), 132.6 (dd, $^{1}J_{CP}$ = 65.3 Hz, $^{3}J_{CP}$ = 2.2 Hz; C_{PPh}), 133.2 (d, J_{CP} = 6.6 Hz; CH_{PPh}), 133.6 (d, J_{CP} = 9.8 Hz; CH_{PPh}), 133.8 (d, J_{CP} = 16.9 Hz; CH_{PPh}), 134.2 (dd, $^{1}J_{CP}$ = 95.4 Hz, $^{3}J_{CP}$ = 2.9 Hz; C_{PPh}), 134.5 (dd, $^{1}J_{CP}$ = 74.8 Hz, $^{3}J_{CP}$ = 3.1 Hz; C_{PPh}), 134.9−135.4 (br; CH_{PPh}), 135.3 (d, J_{CP} = 8.4 Hz; CH_{PPh}), 137.3 (d, J_{CP} = 10.1 Hz; CH_{PPh}), 138.7 (d, J_{CP} = 15.4 Hz; CH_{PPh}), 140.2 ($C_{Tol,\ para}$), 145.5 ($CH_{Tol,\ ipso}$), 146.6 (dd, $^{2}J_{CP}$ = 19.1 Hz, $^{2}J_{CP}$ = 10.1 Hz; *C*Ir). $^{31}P\{^{1}H\}$ NMR (162.1 MHz, CD_2Cl_2, −30 °C): δ = −2.9 (d, $^{2}J_{PP}$ = 65.7 Hz), 27.5 (d, $^{2}J_{PP}$ = 65.7 Hz). Anal. Calcd for $C_{46}H_{44}O_2P_2SClIr$: C, 58.13; H 4.67; S, 3.37. Found: C, 58.38; H 4.64; S, 3.03

X-ray Crystallographic Studies. Data collection of all compounds was conducted either with a Bruker X8-APEX II (**1**·$Ni(CO)_3$, **1**·$Ni(CO)_2$, **1**·Pd(allyl)Cl, **1**·Rh(CO)Cl, **5**) or a Rigaku XtaLAB Synergy (**1**, **3**, [**4a**][BF_4], [PPN][**4b**], **6**). Suitable crystals of all compounds were mounted in an inert oil (perfluoropoly alkylether) and directly transferred into a cold nitrogen stream. Crystal structure determinations were affected at 100 K. The structures were solved using direct methods, refined using full-matrix least-squares techniques on F^2 with the Shelx software package[21] and expanded using Fourier techniques. Data collection parameters are given in Tables S1−S4. Crystallographic data (including structure factors) have been deposited with the Cambridge Crystallographic Data Centre as supplementary publication no. CCDC-1906068−1906077.

■ ASSOCIATED CONTENT

Supporting Information

The Supporting Information is available free of charge on the ACS Publications website at DOI: 10.1021/acs.inorgchem.9b00948.

NMR spectra, crystallographic information, and structures (PDF)

Accession Codes

CCDC 1906068−1906077 contain the supplementary crystallographic data for this paper. These data can be obtained free of charge via www.ccdc.cam.ac.uk/data_request/cif, or by emailing data_request@ccdc.cam.ac.uk, or by contacting The Cambridge Crystallographic Data Centre, 12 Union Road, Cambridge CB2 1EZ, UK; fax: +44 1223 336033.

■ AUTHOR INFORMATION

Corresponding Author

*(V.H.G.) E-mail: viktoria.gessner@rub.de.

ORCID

Viktoria H. Gessner: 0000-0001-6557-2366

DOI: 10.1021/acs.inorgchem.9b00948
Inorg. Chem. 2019, 58, 8151−8161

Author Contributions

The manuscript was written through contributions of V.H.G. and T.S. All authors have given approval to the final version of the manuscript. T.S. has performed most of the synthetic work and all the crystallographic studies. I.R. and M.P. performed some reactions.

Funding

This project has received funding from the European Research Council under the European Union's Horizon 2020 research and innovation program (Grant Agreement No. 677749).

Notes

The authors declare no competing financial interest.

REFERENCES

(1) For reviews: (a) Gillespie, J. A.; Dodds, D. L.; Kamer, P. C. J. Rational design of diphosphorus ligands − a route to superior catalysts. *Dalton Trans.* **2010**, *39*, 2751. (b) Allen, D. W. Phosphines and related P−C-bondedcompounds. *Organophosphorus Chem.* **2014**, *43*, 1.

(2) For examples: (a) Gracia, C.; Marco, G.; Navarro, R.; Romero, P.; Soler, T.; Urriolabeitia, E. P. C-P and C-H Bond Activations and C-C Coupling in Bis-Phosphonium Salts Induced by Platinum(II) Complexes. *Organometallics* **2003**, *22*, 4910. (b) Fujita, K.-i.; Nakaguma, H.; Hamada, T.; Yamaguchi, R. Inter- and Intramolecular Activation of Aromatic C−H Bonds by Diphosphine and Hydrido-Bridged Dinuclear Iridium Complexes. *J. Am. Chem. Soc.* **2003**, *125* (41), 12368−12369. (c) Cooper, A. C.; Clot, E.; Huffman, J. C.; Streib, W. E.; Maseras, F.; Eisenstein, O.; Caulton, K. G. Computational and Experimental Test of Steric Influence on Agostic Interactions: A Homologous Series for Ir(III). *J. Am. Chem. Soc.* **1999**, *121* (1), 97−106. (d) Chakravarty, A. R.; Cotton, F. A.; Tocher, D. A. ortho-Metallation at dimetallic centres: syntheses and X-ray characterization of $Os_2(O_2CMe)_2[Ph_2P(C_6H_4)]Cl_2$ and $Rh_2(O_2CMe)_2[Ph_2P(C_6H_4)]_2(2MeCO_2H)$. *J. Chem. Soc., Chem. Commun.* **1984**, *0*, 501−502.

(3) For recent examples, see: (a) Foley, B. J.; Palit, C. M.; Timpa, S. D.; Ozerov, O. V. Synthesis of (POCOP)Co(Ph)(X) Pincer Complexes and Observation of Aryl−Aryl Reductive Elimination Involving the Pincer Aryl. *Organometallics* **2018**, *37* (21), 3803−3812. (b) Lekich, T. T.; Gary, J. B.; Bellows, S. M.; Cundari, T. R.; Guard, L. M.; Heinekey, D. M. H_2 addition to (^{Me4}PCP)Ir(CO): studies of the isomerization mechanism. *Dalton. Trans.* **2018**, *47*, 16119−16125. (c) Li, Y.; Krause, J. A.; Guan, H. Cobalt POCOP Pincer Complexes via Ligand C−H Bond Activation with $Co_2(CO)_8$: Catalytic Activity for Hydrosilylation of Aldehydes in an Open vs a Closed System. *Organometallics* **2018**, *37* (13), 2147−2158. (d) Vlahopoulou, G.; Möller, S.; Haak, J.; Hasche, P.; Drexler, H.-J.; Heller, D.; Beweries, T. Synthesis of Rh(III) thiophosphinito pincer hydrido complexes by base-free C−H bond activation at room temperature. *Chem. Commun.* **2018**, *54*, 6292−6295. (e) Hoffbauer, M. R.; Comanescu, C. C.; Dymm, B. J.; Iluc, V. M. Influence of the Leaving Group on C−H Activation Pathways in Palladium Pincer Complexes. *Organometallics* **2018**, *37*, 2086. (f) Gloaguen, Y.; Jongens, L. M.; Reek, J. N. H.; Lutz, M.; de Bruin, B.; van der Vlugt, J. I. Reductive Elimination at an Ortho-Metalated Iridium(III) Hydride Bearing a Tripodal Tetraphosphorus Ligand. *Organometallics* **2013**, *32*, 4284. (g) Campos, J.; Espada, M. F.; López-Serrano, J.; Carmona, E. Cyclometalated Iridium Complexes of Bis(Aryl) Phosphine Ligands: Catalytic C−H/C−D Exchanges and C−C Coupling Reactions. *Inorg. Chem.* **2013**, *52*, 6694.

(4) For reviews: Peris, E.; Crabtree, R. H. Key factors in pincer ligand design. *Chem. Soc. Rev.* **2018**, *47*, 1959−1968. (b) Albrecht, M.; van Koten, G. Platinum Group Organometallics Based on "Pincer" Complexes: Sensors, Switches, and Catalysts. *Angew. Chem., Int. Ed.* **2001**, *40* (20), 3750−3781. (c) van der Boom, M. E.; Milstein, D. Cyclometalated Phosphine-Based Pincer Complexes: Mechanistic Insight in Catalysis, Coordination, and Bond Activation. *Chem. Rev.* **2003**, *103* (5), 1759−1792.

(5) (a) de la Torre, G.; Gouloumis, A.; Vázquez, P.; Torres, T. Insights into the Aryl−Aryl Exchange between Palladium and Phosphane Ligands in PdII Complexes: Preparation of Phthalocyanine-Containing Phosphonium Salts. *Angew. Chem., Int. Ed.* **2001**, *40*, 2895. (b) Goodson, F. E.; Wallow, T. I.; Novak, B. M. Mechanistic Studies on the Aryl-Aryl Interchange Reaction of $ArPdL_2I$ (L = Triarylphosphine) Complexes. *J. Am. Chem. Soc.* **1997**, *119*, 12441. (c) Kong, F. Y.; Cheng, K. S. Facile Aryl-Aryl Exchange between the Palladium Center and Phosphine Ligands in Palladium(II) Complexes. *J. Am. Chem. Soc.* **1991**, *113*, 6313.

(6) (a) Kwong, F. Y.; Chan, K. S. Synthesis of Biaryl P,N Ligands by Novel Palladium-Catalyzed Phosphination Using Triarylphosphines: Catalytic Application of C-P Activation. *Organometallics* **2000**, *19*, 2058. (b) Kwong, F. Y.; Chan, K. S. A general synthesis of aryl phosphines by palladium catalyzed phosphination of aryl bromides using triarylphosphines. *Chem. Commun.* **2000**, 1069. (c) Zhang, X.; McNally, A. Phosphonium Salts as Pseudohalides: Regioselective Nickel-Catalyzed Cross-Coupling of Complex Pyridines and Diazines. *Angew. Chem., Int. Ed.* **2017**, *56*, 9833.

(7) Scherpf, T.; Schwarz, C.; Scharf, L. T.; Zur, J.-A.; Helbig, A.; Gessner, V. H. Ylide-functionalized phosphines: Strong Donor Ligands for Homogenous Catalysis. *Angew. Chem.* **2018**, *130*, 13041.

(8) For other examples of electron-rich phosphine ligands see: (a) Wünsche, M. A.; Mehlmann, P.; Witteler, T.; Buß, F.; Rathmann, P.; Dielmann, F. Imidazolin-2-ylidenaminophosphines as Highly Electron-Rich Ligands for Transition-Metal Catalysts. *Angew. Chem., Int. Ed.* **2015**, *54*, 11857. (b) Ackermann, L.; Born, R. Modular Diamino and Dioxophosphine Oxides and Chlorides as Ligands for Transition-Metal-Catalyzed C-C and C-N Couplings with Aryl Chlorides. *Angew. Chem., Int. Ed.* **2005**, *44*, 2444. (c) Martin, D.; Moraleda, D.; Achard, T.; Giordano, L.; Buono, G. Assessment of the Electronic Properties of P ligands Stemming from Secondary Phosphine Oxides. *Chem. - Eur. J.* **2011**, *17*, 12729. (d) Chen, L.; Ren, P.; Carrow, B. P. *J. Am. Chem. Soc.* **2016**, *138*, 6392.

(9) Weber, P.; Scherpf, T.; Rodstein, I.; Lichte, D.; Scharf, L. T.; Gooßen, L. J.; Gessner, V. H. A Highly Active Ylide-Functionalized Phosphine for Palladium-Catalyzed Aminations of Aryl Chlorides Ylide-functionalized phosphines: Strong Donor Ligands for Homogenous Catalysis. *Angew. Chem., Int. Ed.* **2019**, *58*, 3203.

(10) (a) Barder, T. E.; Biscoe, M. R.; Buchwald, S. L. Structural Insights into Active Catalyst Structures and Oxidative Addition to (Biaryl)phosphine-Palladium Complexes via Density Functional Theory and Experimental Studies. *Organometallics* **2007**, *26*, 2183−2192. (b) Barder, T. E.; Buchwald, S. L. Insights into Amine Binding to Biaryl Phosphine Palladium Oxidative Addition Complexes and Reductive Elimination from Biaryl Phosphine Arylpalladium Amido Complexes via Density Functional Theory. *J. Am. Chem. Soc.* **2007**, *129*, 12003−12010. (c) Yamashita, M.; Takamiya, I.; Jin, K.; Nozaki, K. Syntheses and characterizations of methylpalladium complexes bearing a biphenyl-based bulky phosphine ligand: Weak interactions suggested by NBO and QTAIM analyses. *J. Organomet. Chem.* **2006**, *691*, 3189−3195.

(11) (a) D'yachihin, D. I.; Dolgushin, F. M.; Godovikov, I. A.; Chizhevsky, I. T. Synthesis and characterization of isomeric 4- and 8-(σCH = CHPh)-*closo*-ruthenacarboranes with η^3:η^2-phosphacarbocyclic ligand. *J. Organomet. Chem.* **2011**, *696*, 3846. (b) Kuwabara, T.; Kato, T.; Takano, K.; Kodama, S.; Manabe, Y.; Tsuchida, N.; Takano, K.; Minami, Y.; Hiyama, T.; Ishii, Y. P−C reductive elimination in Ru(II) complexes to convert triarylphosphine ligands into five- or six-membered phosphacycles. *Chem. Commun.* **2018**, *54*, 5357. (c) Lindenberger, H.; Birk, R.; Orama, O.; Huttner, G.; Berke, H. Ketenylidentriphenylphosphoran-Komplexe, *Z. Z. Naturforsch., B: J. Chem. Sci.* **1988**, *43b*, 749.

(12) (a) Münchenberg, J.; Fischer, A. K.; Thönnessen, H.; Jones, P. G.; Schmutzler, R. *N*-(*N*′,*N*′,*N*″,*N*″-tetramethyl)guanidine-substituted phosphines as monodentate, bidentate or tridentate ligands in transition metal chemistry. *J. Organomet. Chem.* **1997**, *529*, 361−

DOI: 10.1021/acs.inorgchem.9b00948
Inorg. Chem. 2019, 58, 8151−8161

374. (b) Pickardt, J.; Rösch, L.; Schumann, H. Die Kristallstruktur von Pentacarbonyl(tri-tert-butylphosphin)wolfram und Tricarbonyl-(tri-tert-butylphosphin)nickel. *Z. Anorg. Allg. Chem.* **1976**, *426* (1), 66−76. (c) Gudat, D.; Bajorat, V.; Häp, S.; Nieger, M.; Schröder, G. Reduction of Bis(phosphonio)isophosphindolides to Phosphane-Functionalized Benzo[c]phospholides. *Eur. J. Inorg. Chem.* **1999**, *1999* (7), 1169−1174.

(13) (a) Paul, U. S. D.; Radius, U. Synthesis and Reactivity of Cyclic (Alkyl)(Amino)Carbene Stabilized Nickel Carbonyl Complexes. *Organometallics* **2017**, *36*, 1398. (b) Paul, U. S. D.; Sieck, C.; Haehnel, M.; Hammond, K.; Marder, T. B.; Radius, U. Cyclic (Alkyl)(Amino)Carbene Complexes of Rhodium and Nickel and Their Steric and Electronic Parameters. *Chem. - Eur. J.* **2016**, *22*, 11005. (c) Marín, M.; Moreno, J. J.; Navarro-Gilabert, C.; Álvarez, E.; Maya, C.; Peloso, R.; Nicasio, M. C.; Carmona, E. Synthesis, Structure and Nickel Carbonyl Complexes of Dialkylterphenyl Phosphines. *Chem. - Eur. J.* **2019**, *25*, 260.

(14) (a) Tolman, C. A. Electron Donor-Acceptor Properties of Phosphorus Ligands. Substituent Additivity. *J. Am. Chem. Soc.* **1970**, *92*, 2953−2956. (b) Huynh, H. V. Electronic Properties of N-Heterocyclic Carbenes and Their Experimental Determination. *Chem. Rev.* **2018**, *118* (19), 9457−9492.

(15) For examples, see: (a) Duncan, J. A. S.; Hedden, D.; Roundhill, D. M.; Stephenson, T. A.; Walkinshaw, M. D. Synthesis of Novel Iridium and Rhodium Complexes Containing Diphenylphosphinito and Dimethylphosphito Ligands. *Angew. Chem., Int. Ed. Engl.* **1982**, *21* (6), 452−453. (b) Suzuki, T.; Isobe, K.; Kashiwabara, K.; Fujita, J.; Kaizaki, S. Preparation and characterization of rhodium(III) complexes containing 1,1,1-tris(dimethyl−phosphinomethyl)−ethane (tdmme). Structures of $[RhX_3(tdmme)]$(X = Cl, Br or I), $[Rh(NH_3)_3(tdmme)]^{3+}$ and $[\{Rh(tdmme)\}_2(\mu\text{-}X)_3]^{3+}$ (X = Cl or OH) in the solid state and in solution. *J. Chem. Soc., Dalton Trans.* **1996**, *0*, 3779−3786. (c) Cotton, F. A.; Kang, S. J. Preparation and structure of rhodium phosphine compounds containing the [Rh2 × 7(PR3)2]- anion and their stereospecific reactions with phosphines to produce [Rh2 × 7(PR3)3]- species. *Inorg. Chem.* **1993**, *32* (11), 2336−2342. (d) Rechavi, D.; Scopelliti, R.; Severin, K. The Enigmatic Nature of $Rh^{I}Cl$(cyclopentadienone) Complexes: Dimers, Trimers, and Tetramers. *Organometallics* **2008**, *27* (22), 5978−5983.

(16) For example: (a) Böttcher, H.-C.; Mayer, P. Convenient Synthesis and Molecular Structure of the CyclometallatedComplex $[IrCl(H)(C_6H_4PPh_2)(PPh_3)_2]$. *Z. Naturforsch., B: J. Chem. Sci.* **2014**, *69b*, 1237−1240. (b) Adams, J. J.; Lau, A.; Arulsamy, N.; Roddick, D. M. Acceptor PCP Pincer Iridium Chemistry: $(^{CF3}PCP)Ir^{III}$ Coordination Properties. *Organometallics* **2011**, *30*, 689−696. (c) Lai, R.-Y.; Surekha, K.; Hayashi, A.; Ozawa, F.; Liu, Y.-H.; Peng, S.-M.; Liu, S.-T. Intra- and Intermolecular Hydroamination of Alkynes Catalyzed by *ortho*-Metalated Iridium Complexes. *Organometallics* **2007**, *26*, 1062−1068.

(17) Scherpf, T.; Wirth, R.; Molitor, S.; Feichtner, K.-S.; Gessner, V. H. Bridging the Gap between Bisylides and Methandiides: Isolation, Reactivity, and Electronic Structure of an Yldiide. *Angew. Chem., Int. Ed.* **2015**, *54*, 8542.

(18) Giordano, G.; Crabtree, R. H.; et al. Di-μ-chloro-bis(η4−1,5-cyclooctadiene)dirhodium(I). *Inorg. Synth.* **1990**, *28*, 88−90.

(19) Ensign, S. C.; Vanable, E. P.; Kortman, G. D.; Weir, L. J.; Hull, K. L. Anti-Markovnikov Hydroamination of Homoallylic Amines. *J. Am. Chem. Soc.* **2015**, *137*, 13748−13751.

(20) Hieber, W.; Fischer, E. O.; Böckly, E. Über Metallcarbonyl. 53. Neue Laboratoriumsmethoden zur Darstellung der Carbonyle von Nickel und Kobalt. *Z. Anorg. Allg. Chem.* **1952**, *269*, 308−316.

(21) (a) Sheldrick, G. A short history of SHELX. *Acta Crystallogr., Sect. A: Found. Crystallogr.* **2008**, *64* (1), 112−122. (b) Sheldrick, G. Crystal structure refinement with SHELXL. *Acta Crystallogr., Sect. C: Struct. Chem.* **2015**, *71* (1), 3−8.

DOI: 10.1021/acs.inorgchem.9b00948
Inorg. Chem. 2019, 58, 8151−8161